

Density-functional study of the evolution of the electronic structure of oligomers of thiophene: Towards a model Hamiltonian

R. Telesca,¹ H. Bolink,² S. Yunoki,³ G. Hadziioannou,² P. Th. Van Duijnen,¹ J. G. Snijders,¹ H. T. Jonkman,³ and G. A. Sawatzky³

¹*Department of Theoretical Chemistry, Material Science Center, University of Groningen, Nijenborgh 4, 9747 AG Groningen, The Netherlands*

²*Department of Polymer Chemistry, Material Science Center, University of Groningen, Nijenborgh 4, 9747 AG Groningen, The Netherlands*

³*Department of Solid State Physics, Material Science Center, University of Groningen, Nijenborgh 4, 9747 AG Groningen, The Netherlands*

(Received 19 July 2000; published 30 March 2001)

We present density-functional and time-dependent density-functional studies of the ground, ionic, and excited states of a series of oligomers of thiophene. We show that, for the physical properties, the most relevant highest occupied and lowest unoccupied molecular orbitals develop gradually from monomer molecular orbitals into occupied and unoccupied broad bands in the large length limit. We show that band gap and ionization potentials decrease with size, as found experimentally and from empirical calculations. This gives credence to a simple tight-binding model Hamiltonian approach to these systems. We demonstrate that the length dependence of the experimental excitation spectra for both singlet and triplet excitations can be very well explained with an extended Hubbard-like Hamiltonian, with a monomer on-site Coulomb and exchange interaction and a nearest-neighbor Coulomb interaction. We also study the ground and excited-state electronic structures as functions of the torsion angle between the units in a dimer, and find almost equal stabilities for the *transoid* and *cisoid* isomers, with a transition energy barrier for isomerization of only 4.3 kcal/mol. Fluctuations in the torsion angle turn out to be very low in energy, and therefore of great importance in describing even the room-temperature properties. At a torsion angle of 90° the hopping integral is switched off for the highest occupied molecular orbital levels because of symmetry, allowing a first-principles estimate of the on-site interaction minus the next-neighbor Coulomb interaction as it enters in a Hubbard-like model Hamiltonian.

DOI: 10.1103/PhysRevB.63.155112

PACS number(s): 71.15.Ap, 71.15.Mb, 78.30.Jw

I. INTRODUCTION

Oligomers consist of monomer units coupled together to form small chain length polymers. They are highly interesting because of many potential applications in electronic and optoelectronic devices. Recently bulk heterojunction, photovoltaic cells,¹ light-emitting diodes² and field-effect transistors³ have been demonstrated with oligomers of thiophene as one of the active components. Because of their interesting optoelectronic charge generating and charge transporting properties, there is considerable interest in the basic electronic structure of the oligomers and the fundamental interactions, which determine the charge- and spin-density distributions in the ground, ionized, and excited states of these systems.^{4,5} There are still strong debates concerning the importance of the electron-electron interactions, electron-vibronic coupling, the size of the bandwidths in large systems, the influence of torsion motions, and the coupling with electronic degrees of freedom which determine the existence and spatial extent of excitonic states, the localization lengths of excitations, the mobility of charge carriers in a single strand polymer, the optical oscillator strengths, and the ionization potentials. Many of the physical properties of π -conjugated systems, of which polyacetylene is the most used example, can be very well explained within the Su-Schrieffer-Heeger (SSH) model,⁶ in which the electronic structure is modeled according to that of one-dimensional

strongly dimerized chain of units with one orbital of importance per unit. This models the alternation of double and single bonds in polyacetylene and, with two electrons per dimer, this results in a semiconducting material. In the SSH model the electron-lattice coupling is considered to be very strong, resulting in a strong polarization of the lattice around the free charge carriers in the valence or conduction bands. Moreover, because of the conjugated nature of these systems, the actual charges and spins are bound to antiphase domain boundaries in the lattice alternation, and move as free solitons along the chain. In this model the electron-electron interactions are neglected, so that the first excited states are expected to be charged polarons or solitons rather than locally charge neutral excitons, as expected for strong local Coulomb interactions. This model is also often applied to the thiophenes, which have an electronic structure as depicted in Fig. 1, where we highlight the backbone, which looks like polyacetylene. However the sulfur atom in each monomer breaks the symmetry present in polyacetylene, thereby removing the twofold degeneracy of the ground state and creating, as a consequence, quite a different system than polyacetylene. In the past two decades a large number of experimental and theoretical studies of the ground and excited states of thiophene and its oligomers has been published, and these were reviewed in a recent book edited by Denis Fichou.⁵ An important contribution in gaining more fundamental insight into the electronic structure of oligomers and polymers has been in the formulation of effective low-

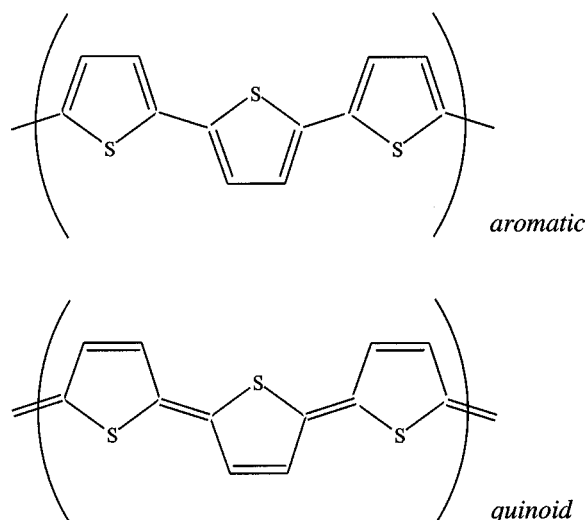


FIG. 1. Schematic structure of the oligothiophenes. The energetically nongenerate isomeric *aromatic* and *quinoid* structures are displayed.

energy models. For example Mintmire and White⁷ came to a first-principles estimate of the optical spectra of polyacetylene within an Ehrenreich-Cohen approach; in other studies^{8,9} a Pariser-Parr-Pople (PPP)-type Hamiltonian with an exciton basis set was used, which allowed them to characterize the excited states, and which gives a better understanding of the photo physics of these materials. Soos *et al.*¹⁰ used exact PPP results to describe the excited state structure of oligomers. Van der Horst *et al.*¹¹ studied the electronic and optical excitations of polythiophene using the GW (G stands for one-electron Green function, W for the screened Coulomb interaction) approximation for the electronic self-energy, and included excitonic effects by solving the electron-hole Bethe-Salpeter equations. Recently a detailed study of the polymer poly phenylene vinylene (PPV) was published using density-functional methods and the GW approximation for the self-energy.¹² The calculated optical spectra suggest very strong electron-hole Coulomb interactions, resulting in strongly bound excitonic states and a large splitting of the singlet and triplet excitons. In our study presented here on the oligomers of thiophene, we will come to similar conclusions concerning the importance of the Coulomb interactions.

Various forms of optical spectroscopy together with theoretical interpretations have provided us with the location of the lowest-energy singlet excitations,^{13–26} as well as in some cases the triplets.²⁷ As we will discuss below, the lowest-energy singlet excitations show a $1/N$ -like dependence (with N the number of rings) on the oligomer length, whereas the lowest triplets are considerably lower in energy. This is already an indication of a relatively strong electron-electron interaction, which, at least for triplet excitations, forms an excitonic state with the electron and hole in proximity to the same monomer, reminiscent of a Frenkel-like limit for the exciton. This in itself requires an effective electron-hole interaction of the order of the one electron bandwidth in the limit of large N .

The lowest singlet excitation seems to be much closer to

the band edge corresponding to the dissociated electron-hole continuum, which is also the conductivity gap. Actually we are not aware of data really pinning down the conductivity gap in the large- N limit. Photoemission studies in the gas phase provide us with accurate values for the ionization potentials which, as the lowest singlet excitations, decrease like $1/N$ with the oligomer size and are in fact well described by a simple tight-binding or Hückel-like model for the molecular-orbital splitting with system size.²¹ It is also interesting to note that the two-photon lowest-energy singlet excitation was expected by the authors of Ref. 22 to cross below the lowest singlet optical excitation for $N > 6$, possibly another strong indication of the importance of electron-electron interactions.

In this paper we present the results of a density-functional calculation of the electronic structure up to lengths of $N = 8$. The advantage is that density-function theory (DFT) is at least in principle exact for determining the ground-state properties of the molecules and ions, and also can be applied to very large systems. In order to study the excited states we used the time-dependent density-functional theory (TDDFT) method, that can then be compared to the excitation energies derived from the occupied and unoccupied orbital energies obtained from the DFT calculation. A strong difference between ionization energies and excitation energies derived from the DFT and the Δ SCF self-consistent-field calculations for the ionization potentials as well as the TDDFT calculations of the excitation energies is again indicative of the importance of electron correlation effects in describing the system. These results are in fact consistent with *ab initio* calculations of small systems, and also with the semiempirical calculations mentioned above, as well as with the experimentally determined energies where available. This exhibits the power of these methods, which can be applied to large systems and are not dependent on empirical parameters. In addition to this, we also study the theoretical optical oscillator strengths using TDDFT theory and the development of these with system size. In each case we interpret the results in terms of simplified models, which can serve as a basis for model Hamiltonians used to describe these systems.

Another aspect, which turns out to be very interesting, is the energy of rotational disorder and the influence of this on the electronic structure and optical properties. For this we studied the ground and excited states of bithiophene (α -2T) as functions of the dihedral angle between the monomer units. Fluctuations in the dihedral angle turn out to be very low in energy, and therefore of great importance in describing even room-temperature properties. Not only is the energy cost low for such excitations, but the electronic structure and optical properties are also strongly dependent on such fluctuations, indicating a strong electron librational coupling.

It is also interesting that for a dihedral angle of 90° the monomer molecular orbitals, which determine the low-energy properties, are completely decoupled, i.e. the hopping integrals are zero for the highest occupied molecular-orbital (HOMO)-based orbitals of the dimer. This gives us a direct handle to calculate the energy of a monomer-monomer charge-transfer excitation, which, when compared to the excitation energy on a single monomer, gives us an *ab initio* measure of the difference between the on-site and nearest-

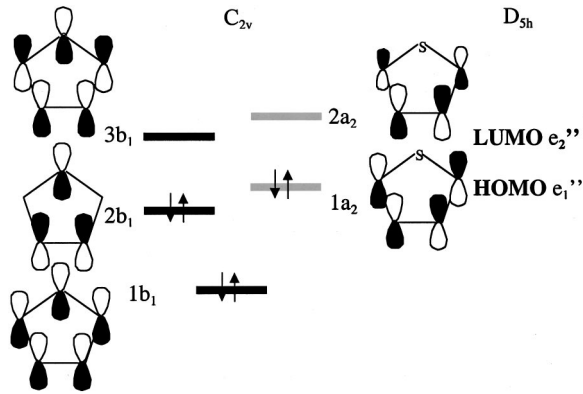


FIG. 2. Energy scheme of the low-energy occupied and unoccupied π orbitals of the thiophene molecule. In this figure the phase and amplitude of the wave functions are indicated.

neighbor Coulomb interactions in an extended Hubbard-like model Hamiltonian. In this way we arrive at what we think is a reliable *ab initio* estimate of all the electronic parameters needed for such a model Hamiltonian, including the coupling to dihedral rotational modes. The coupling with the molecular vibration modes can in principle also be calculated in this way, but remains a subject for future studies. However reasonable estimates of these can also be obtained from the optical¹⁵ and photoelectron spectra presented here.

Before presenting the results, we look at some of the basic information concerning the monomers, which will turn out to be important in describing what happens as we increase N in the oligomers. In Fig. 2 we represent the symmetries and molecular-orbital buildup for the π orbitals of the thiophene molecule. We immediately note that the problem is more complicated than the molecular-orbital structure of the monomer considered in polyacetylene. The most important thing here is that the molecular orbital of the HOMO ($1a_2$) and the lowest unoccupied molecular orbital (LUMO) ($3b_1$) have quite different compositions, and originate from different symmetries. So the HOMO, which can be characterized as an *aromatic* molecular orbital, and will turn out to form a valence band in the oligomer, has no density on the sulfur atom because of symmetry. However, the LUMO, which can be classified as a *quinoid* is in this regard quite strongly coupled to sulfur p - π orbitals. Since the LUMO of the monomer develops into the conduction-band states in the large oligomer limit, we see that the valence and conduction bands are derived from strongly different monomer molecular orbitals. This means that any model Hamiltonian approach should contain at least two different bands, quite different from the two bands one would obtain in a Peierls-distorted one-band system as proposed for polyacetylene.

Another point of great importance is that the HOMO has a large component on the α carbon atom, which is involved in the bonding between the monomers in the oligomer, so that the effective hopping integrals will be large. Surprisingly enough, despite the strong difference in character between the HOMO and LUMO, the effective hopping integrals are of the same magnitude, resulting in similar valence- and conduction-band-widths in the large size limit. We also note that the sign of the hopping integral will be opposite for

the valence and conduction bands, leading to a band structure with the minimum direct gap at $k=0$. Also, the intermonomer mixing of the HOMO and LUMO to the left and right monomers of a central monomer will have opposite signs, and will therefore cancel at $k=0$.

Another complicating factor is the close proximity of the HOMO-1 ($2b_1$) and the LUMO+1 ($2a_2$) to the HOMO and LUMO, respectively. This is because it will turn out that the intermonomer molecular-orbital splitting of the HOMO is much larger than that of the HOMO-1, which has negligible electron density on the α carbon atom positions, so that the $2b_1$ -derived states remain close to the center of the valence band, which could have very important consequences for the optical properties of the oligomers at somewhat higher energies. For the LUMO this is a minor problem, because here the splitting between the $3b_1$ and $2a_2$ orbitals is larger than the expected conduction-band-width, so that the $2a_2$ -derived states remain outside of the conduction-band states or nearly so. We should note, however, that the $2a_2$ molecular orbital has considerable density on the α carbon and therefore will develop a considerable bandwidth, although this turns out to be smaller than the bands derived from the HOMO or LUMO. Of course the really low-energy scale properties at an energy scale of the band gap in the larger length oligomers will not be influenced much by these other molecular orbitals, but they will be important for higher-energy excitations. We now have a good basis for discussing DFT and TDDFT calculations on the oligomers.

II. THEORY

In order to gain insight into the nature of the ground, ionized and excited states of thiophene oligomers as function of their chain length, we analyzed their electronic structure applying (time-dependent) density-functional theory to these systems, implemented by the Amsterdam Density Functional Program Package (ADF),²⁸⁻³⁰ which is able to provide accurate solutions of the Kohn-Sham (KS) equations even for fairly long oligomers. In the ground-state calculations we used the local-density approximation, based on the parameterization of the electron gas data given by Vosko, Wilk and Nusair.³¹ The basis sets used were of triple zeta plus polarization Slater-type orbital function quality (basis IV in the ADF). Excited states were calculated using time-dependent density-functional theory³² as implemented in the RESPONSE part of the ADF.³²⁻³⁴ Since TDDFT describes (in principle exactly) how the electron density changes in time under the influence of a time-dependent perturbation, and since this time-dependent density will resonate at the exact excitation energies of the system, linear-response theory based on TD-DFT is able to provide both these excitation energies as well as the corresponding oscillator strengths. In practice,³² to calculate excitation energies and oscillator strengths, the following eigenvalue equation has to be solved:

$$\Omega \mathbf{F}_i = \omega_i^2 \mathbf{F}_i, \quad (1)$$

where the four-index matrix Ω has components given by

$$\Omega_{ia\sigma,jb\tau} = \delta_{\sigma\tau}\delta_{ij}\delta_{ab}(\varepsilon_{a\sigma} - \varepsilon_{i\sigma})^2 + 2\sqrt{(\varepsilon_{a\sigma} - \varepsilon_{i\sigma})(\varepsilon_{b\tau} - \varepsilon_{j\tau})}K_{ia\sigma,jb\tau}. \quad (2)$$

Here squared differences between occupied and virtual KS orbital energies (a and b refer to unoccupied energies and i and j to occupied energies, while σ and τ are spin indices) are included and as well as a coupling K matrix, containing Coulomb and exchange-correlation (XC) parts. The square of the desired excitation energies are the eigenvalues ω_i^2 , while the oscillator strengths are simply related to the eigenvectors F_i . Note that the elements of the eigenvectors F_i are roughly comparable to the configuration interaction coefficients in a singly excited configuration-interaction calculation, and are a measure to what extent the corresponding excitation can be interpreted as a pure single-particle excitation or if several such excitations play a crucial role in the transition. The Coulomb part of the coupling matrix is given by

$$K_{lj\sigma,kl\tau}^{\text{Coul}} = \int d\mathbf{r} \int d\mathbf{r}' \phi_{i\sigma}(\mathbf{r})\phi_{j\sigma}(\mathbf{r}) \times \frac{1}{|\mathbf{r} - \mathbf{r}'|} \phi_{k\tau}(\mathbf{r}')\phi_{l\tau}(\mathbf{r}'), \quad (3)$$

while the exchange-correlation part

$$K_{lj\sigma,kl\tau}^{\text{xc}}(\omega) = \int d\mathbf{r} \int d\mathbf{r}' \phi_{i\sigma}(\mathbf{r})\phi_{j\sigma}(\mathbf{r}) \times f_{\text{xc}}^{\sigma\tau}(\mathbf{r}, \mathbf{r}', \varpi) \phi_{k\tau}(\mathbf{r}')\phi_{l\tau}(\mathbf{r}') \quad (4)$$

is related to the so called exchange correlation kernel

$$f_{\text{xc}}^{\sigma\tau}(\mathbf{r}, \mathbf{r}', t - t') = \frac{\delta v_{\text{xc}}^{\sigma}(\mathbf{r}, t)}{\delta \rho_{\tau}(\mathbf{r}', t')}. \quad (5)$$

In the so called adiabatic local-density approximation (ALDA) used here, the exchange-correlation kernel is simply given by

$$f_{\text{xc}}^{\text{ALDA},\sigma\tau}(\mathbf{r}, \mathbf{r}', \varpi) = \delta(\mathbf{r} - \mathbf{r}') \left. \frac{\delta v_{\text{xc}}^{\text{LDA},\sigma}(r, t)}{\delta \rho_{\tau}} \right|_{\rho_{\tau} = \rho_{\sigma,\tau}(r)}. \quad (6)$$

Although the matrix Ω can become quite large, one is usually interested in the lowest few excitations, and then efficient algorithms (such as the Davidson algorithm^{35,36}) can be used that avoid ever having to construct the matrix explicitly.³⁷

To analyze the nature of the important excitations, we performed a so-called fragment analysis, where the molecule is thought to be built from chemically relevant fragments, and all the molecular orbitals are expressed as linear combinations of the molecular orbitals of the constituting fragments (note that this does not change the outcome of the calculation, but is only an analytical tool). In the case of thiophene oligomers, we built the total molecule from identical thiophene monomers (from which the α hydrogen atoms are removed so they are biradicals) and hydrogen atoms

at the end of the chain. We have verified that using identical monomer units (rather than slightly different ones such as in the experimental and optimized geometries) does not influence the results in any significant way. Moreover we will be mainly concerned with π electrons, and it turns out that an exact treatment of the biradical nature of the σ system does not significantly influence the form of the π electrons. For practical reasons we therefore used fragments in which the two spin components of the singly occupied σ orbitals were occupied with half an electron in a spin-restricted calculation. From this fragment analysis we can derive a fragment-orbital-based Mulliken-type population analysis, which is often much more physically illuminating than a population analysis based on the basis function, and is much less basis set dependent. Apart from the orbitals and electron densities, one can also analyze the transition dipole moments for the various excitations in terms of these fragment orbitals, which can shed light on the factors that determine the strength of a particular transition.

III. RESULTS AND DISCUSSION

This discussion will be divided into several parts according to the discussion in Sec. I. We start with a description of the ground-state electronic structure and the corresponding Kohn-Sham orbital energies as a function of the oligomer length. We will use these orbital energies to see if a tight-binding-like model Hamiltonian description with monomer molecular orbitals as basis sets is an acceptable description of the development of the electronic structure, and in this process we will determine the tight-binding parameters required to closely simulate the DFT results. We then look at the TDDFT calculations of the excitation energies and oscillator strengths, and compare these with the experimental data as well as with the orbital energies obtained from the Kohn-Sham orbital energies. We note here that the DFT orbital energies do not include additional relaxation due to the electron-hole interaction in such an excited state, whereas the TDDFT should at least partially include this. Also it is well known that DFT in solid semiconductors yields band gaps considerably lower than the experimental values, so we expect the DFT values of the excitation energies to lie considerably below the experimental and TDDFT values.

We then study the total energy as a function of the dihedral angle for the dimer, and obtain the energy difference of the *transoid* and *cisoid* geometries as well as the energy barrier to go from one to the other. At a dihedral angle of 90° the intermonomer hopping integral of the HOMO and LUMO monomer orbitals goes to zero by symmetry, allowing us to compare the pure intermolecular electron-hole excitations to the on-site monomer excitations in a dimer. From this we can, in principle, extract the difference of the on-site and nearest-neighbor Coulomb interactions which, together with the exchange interaction determined from the singlet-triplet splitting, gives us the full electronic part of an extended two-band Hubbard model description of the oligothiophenes. We will finally use this model Hamiltonian for a systematic study of the excited-state properties as a function of size.

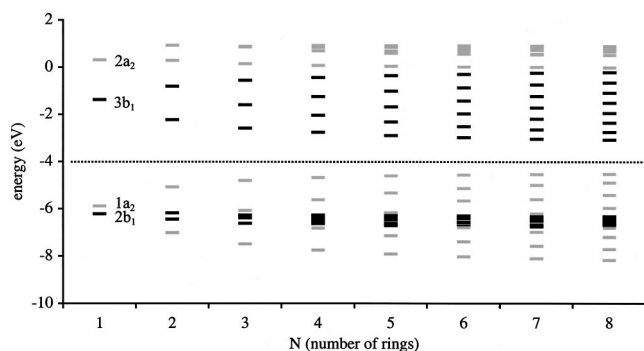


FIG. 3. Developing band structure of the oligomers of thiophene from sizes 1 to 8 as a result of the DFT calculations.

The Kohn-Sham orbital energies obtained from the DFT calculation are plotted as a function of the oligomer length in Fig. 3. We see from Fig. 3 what we anticipated in Sec. I, namely, that the occupied $2b_1$ orbitals hardly “feel” the presence of neighboring monomers and remain sharp molecular levels, while the $1a_2$ orbitals spread out into quite large bandwidth valence bands. Also, the $3b_1$ unoccupied orbitals spread out into bands with widths similar to that of the occupied $1a_2$ -derived band. The $2a_2$ unoccupied orbital also spreads out into a band, but with a width considerably less than the bands derived from $1a_2$ and $3b_1$ molecular orbitals. We note here that the lowest excitation energy obtained from the Kohn-Sham orbital energies is considerably smaller than the experimental lowest singlet excitation energy. At first glance this sounds strange, because the actual excitation energy should be lower in energy because of the possible exciton binding energy, which is not included in the DFT calculation. However, this is a very common and also well-understood problem in semiconductors, and therefore should not really be alarming.

Although we expect that the gap for an electron-hole excitation obtained from the Kohn-Sham orbital energies will be considerably smaller than the experimental gap, we might expect that the relative energies of occupied orbitals as well as unoccupied orbitals would be close to the experimental values. In order to check this, in Fig. 4 we display the gas-phase photoelectron spectrum of the oligomers of thiophene with sizes of 2–6 thiophene units. These spectra were obtained using a home-built photoelectron spectrometer with a specially designed strongly focusing electron lens with a high throughput, in order to collect spectra from a collimated molecular jet beam of the oligomers. These spectra were obtained with HeI radiation of 21.2 eV, and the binding energies were calibrated using the Xe $^2P_{3/2}$ line. These spectra can be directly compared to the molecular-orbital energies of the occupied states as obtained in the DFT calculation.

The spectra exhibit a narrow band at a binding energy between 9.0 and 9.5 eV, which shows only a small change as a function of the size of the oligomer, and is derived from the $2b_1$ HOMO-1 in thiophene, as discussed above. At lower binding energies we see strong changes as function of size, which obviously can be interpreted in terms of the development of the $1a_2$ orbital in thiophene into a rather broad band

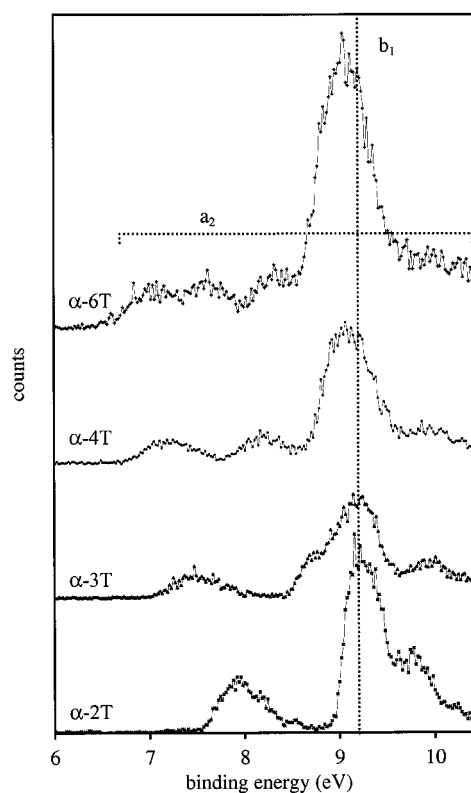


FIG. 4. Gas-phase photoelectron spectra of α -2T, α -3T, α -4T, and α -6T. The $2b_1$ - and $1a_2$ -derived band structures are indicated.

of states corresponding very closely to the development found in the theoretical calculation shown in Fig. 3. In fact what we see is that the $2b_1$ orbital ends up close to the center of the band of states originating from the $1a_2$ orbitals. In Fig. 5(a) we show the dependence of the $1a_2$ -derived bandwidth as a function of oligomer size from both DFT and experiment. The extrapolation to an infinite system yields a bandwidth of $W=3.9$ eV. The solid line drawn in Fig. 5(a) is the theoretical bandwidth based on a two-band tight-binding model, as discussed below. The good agreement with DFT gives us confidence in using the DFT calculations for the unoccupied orbitals, which behave in a manner similar to the occupied $1a_2$ orbitals, ending up with a conduction-bandwidth of about 3.2 eV in the large size limit. This is also shown in Fig. 5(b), together with the tight-binding model calculation discussed below.

In Fig. 6 we display the calculated and experimental ionization potentials as functions of the reciprocal chain length. The experimental ionization potential decreases linearly with the reciprocal chain length. We now compare these values with the ground-state nonrelaxed orbital energies, as obtained in the DFT calculations, although the absolute values differ from the experimental values, as expected they show the same dependence on the reciprocal chain length as the experimental values. DFT calculations on the electronically fully relaxed ionic states (Δ SCF) give results which are numerically closer to the experimental values for the small size oligomers, but underestimate the ionization potentials for the larger size oligomers (Fig. 6). This discrepancy was ex-

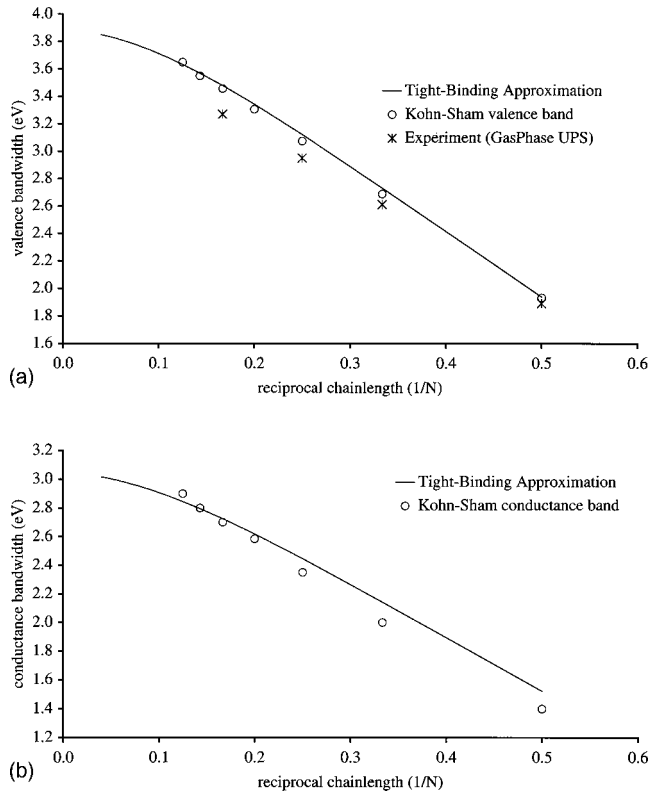


FIG. 5. Valence-band-width (a) and conduction-band-width (b) as functions of the reciprocal chainlength ($1/N$); the open circles represent the results of the DFT calculations, and the solid lines the results of a tight-binding fit with the parameters $t_{hh} = -0.97$ eV, $t_{ll} = 0.76$ eV, and $t_{hl} = 0.30$ eV. For the valence band we plot the values obtained from our gas-phase UPS experiments.

plained in Ref. 38, and can be attributed to an incorrect treatment of the self-energy correction in the density-functional method for charged systems; its value increases with the size of the system.

We note in the experimental photoelectron spectra that the widths of the photoelectron features corresponding to the HOMO in each case are very large indeed. The experimental resolution is 0.1 eV in these scans, which is much smaller

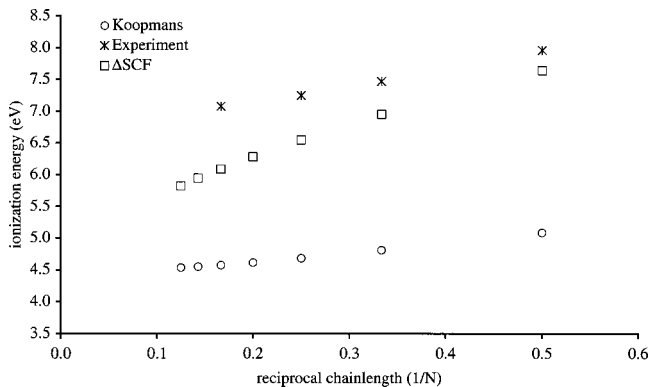


FIG. 6. Comparison between ionization potentials obtained from the gas-phase UPS experiments and the Koopmans and Δ SCF values as obtained from the DFT calculations as functions of the reciprocal chain length ($1/N$).

than the observed widths. This could be due to the electron vibronic coupling, and if this is the case then this coupling strength can be very large indeed. The total spread in energy is about 0.5 eV for the dimer, and increases to 1 eV for α -4T. This increase in width with the system size is not really expected for local electron vibronic coupling, perhaps indicating other possible origins for this broadening. From optical photoluminescence studies it has been found that singlet-singlet transitions are strongly coupled to vibronic modes of various kinds with the 1470-cm^{-1} (C-C stretch) mode dominating. The width of the optical transitions resulting from this is about 0.3 eV.³⁹ Of course this cannot be directly compared with the photoemission width, since the nature of the excited states is different. However, since the widths and shapes are more or less independent of the size of the oligomer in the optical data, this indicates that an additional broadening mechanism is present in the photoelectron spectra. In any case we can conclude from the optical studies that the electron vibronic coupling to the C-C double-bond mode is very strong, and corresponds to an average of two vibrational quanta, which are involved in the electronic relaxation energy due to bond-length changes. As we will discuss below, there are additional broadening mechanisms in the photoelectron spectra, which may originate from the strong change in the intermonomer hopping integrals due to low-energy torsion modes, and the small energy difference between the *cisoid* and *transoid* configurations of the thiophene-thiophene bonds. In fact we suggest that this small energy difference, and the strong influence it has on the electronic structure, is probably the main source of the so-called defect states that seem to dominate the transport properties of the oligomers of thiophene in the solid state.

As seen above, the progression of electronic states corresponding to $1a_2$ and $3b_1$ molecular orbitals with size is reminiscent of a simple tight-binding-like model prediction. As noted by others,²¹ this indicates that the molecular-orbital structure of the monomers stays intact, and all that happens is that the monomer levels develop into broad bands in the long length limit in a way described by introducing nearest-neighbor intermonomer hopping integrals but otherwise leaving everything the same. We already suggested above that the actual model one should use is more complicated than a simple single-band model, since there will be hopping integrals of comparable size, coupling the $1a_2$ - $1a_2(t_{hh})$, $1a_2$ - $3b_1(t_{hl})$, and $3b_1$ - $3b_1(t_{ll})$ molecular orbitals on neighbor monomers. This can be easily concluded from the molecular-orbital structure shown in Fig. 2, and also from the DFT calculations of Fig. 3. In fact it is easy to estimate the relative sizes and also signs of such hopping integrals from the phase and amplitude of the C $2p$ - π wave functions on the two α carbon atoms of the monomer. The fact that the singlet-triplet splitting is large indicates that at least the triplet is an excitonic-like states, which points in the direction of a large monomer on-site Coulomb interaction and also a large exchange interaction. These considerations lead us to propose a two-band extended Hubbard model Hamiltonian describing the electronic properties of these systems,

$$H = H_\varepsilon + H_t + H_u + H_v + H_g, \quad (7a)$$

where

$$H_\varepsilon = \sum_{i=1, \sigma=\uparrow\downarrow}^N \sum_{m=h,l} \varepsilon_m c_{i,\sigma}^{m+} c_{i,\sigma}^m, \quad (7b)$$

$$H_t = \sum_{i=1, \sigma=\uparrow\downarrow}^N \sum_{m=h,l} t_{mm} c_{i,\sigma}^{m+} c_{i+1,\sigma}^m + t_{hl} \times \sum_{i=1, \sigma=\uparrow\downarrow}^N [c_{i,\sigma}^{h+} c_{i+1,\sigma}^l + c_{i,\sigma}^{l+} c_{i+1,\sigma}^h], \quad (7c)$$

$$H_u = \sum_{i=1}^N \left\{ [U + \Delta U (\delta_{i,1} + \delta_{i,N})] \times \left[\sum_{m=h,l} n_{i,m\uparrow} n_{i,m\downarrow} + n_{i,h} n_{i,l} \right] \right\}, \quad (7d)$$

$$H_v = V \left[\sum_{i=1}^N \sum_{m=h,l} n_{i,m} n_{i+1,m} + \sum_{i=1}^N (n_{i,h} n_{i+1,l} + n_{i,l} n_{i+1,h}) \right], \quad (7e)$$

$$H_s = -2K \sum_{i=1}^N \left[\mathbf{S}_i^h \mathbf{S}_i^l + \frac{1}{4} n_i^h n_i^l \right], \quad (7f)$$

and

$$n_{i,m} = n_{i,m\uparrow} + n_{i,m\downarrow},$$

$$n_{i,m\uparrow} = c_{i,\uparrow}^{m+} c_{i,\downarrow}^m. \quad (7g)$$

Here i is the site, and h and l are the HOMO and LUMO, and ε_h and ε_l are the one-electron thiophene HOMO and LUMO energies. U is the on-site Coulomb interaction which we assume to be the same for two electrons in the HOMO, two in the LUMO, and one in the HOMO and one in the LUMO, as long as they are on the same monomer. The Coulomb interaction at the chain ends is taken to be $0.5 \text{ eV} (\Delta U)$ larger than at other positions, because of the reduced coordination number there; therefore, there is a reduced screening of U . V is the nearest-neighbor Coulomb interaction, and K is the exchange integral. A fit of the one-electron part of this Hamiltonian to the DFT calculations leads to the following values for the hopping integrals: $t_{hh} = -0.97 \text{ eV}$, $t_{ll} = 0.76 \text{ eV}$, and $t_{hl} = 0.30 \text{ eV}$ [Figs. 5(a) and 5(b)]. We should note that the Kohn-Sham orbital energies give too small an energy splitting ($\Delta = \varepsilon_h - \varepsilon_l = 4.52 \text{ eV}$ for the monomer) between the $1a_2^-$ and $3b_1^-$ -based bands (Fig. 7); thus to simulate the DFT calculations with the one-electron part of our model Hamiltonian, we must start with a $\Delta\varepsilon$ which is smaller than the experimental value (5.52 eV) in order to obtain a good fit and in order to extract the hopping integrals. Here the mixing of the $1a_2^-$ and $3b_1^-$ -based bands will be smaller than in the DFT calculation because of their larger splittings. The best way to confirm this would be with inverse photoemission, which unfortunately is hard to do in these systems due to reasons of intensity. A detailed electron-energy-loss study, in which one can separate the excitonic and interband

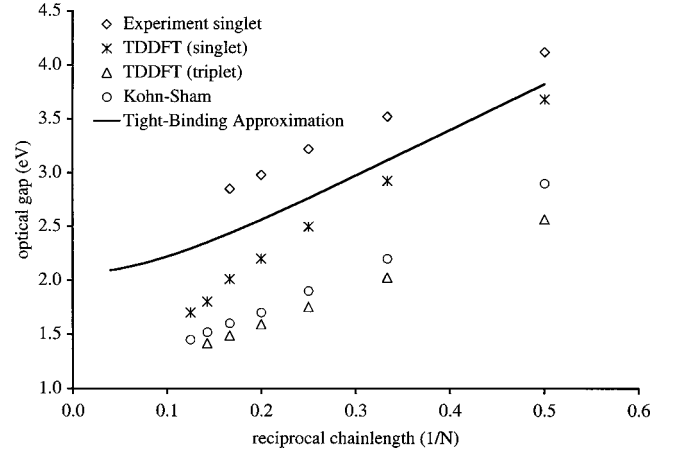


FIG. 7. Singlet optical gap as obtained from DFT and TDDFT calculations as a function of the reciprocal chain length ($1/N$). The results for the triplet optical gap obtained from the TDDFT calculations are also plotted, as well as the experimental singlet results (band maximum) (Ref. 23).

electron-hole transitions by varying the incident energy, may be another way to obtain experimental values for the true gaps.

Before we discuss the determination of these parameter values, we first must have a good understanding of the optical spectra. We now show how the optical spectrum of the oligomers evolves and can be understood from the basic electronic structure of the thiophene monomer by applying simple tight-binding theoretical concepts. Thiophene is iso-electronic with the cyclopentadienyl anion, which has a D_{5h} point group symmetry. The HOMO-LUMO transition ($e_1'' \rightarrow e_2''$) in cyclopentadienyl leads to two excited states; the lowest one, with E_2' symmetry, is strictly forbidden by dipole selection rules, and the second, of E_1' symmetry, is higher in energy but is allowed. If we lower the symmetry to the subgroup C_{2v} without changing the geometry, the degenerate representation E_1' splits into $A_1 + B_2$, and E_2' reduces to $A_1 + B_2$. So, imposing C_{2v} symmetry on cyclopentadienyl, we find that the lowest excitations of A_1 and B_2 symmetry are forbidden, while the next two lowest excitations in both symmetries are allowed. In thiophene the D_{5h} symmetry is slightly broken, so the lowest A_1 and B_2 transitions are now formally allowed (and no longer at exactly the same energy) but in fact still weak. The thiophene HOMO-LUMO transition $1a_2 \rightarrow 3b_1$ is the lowest of B_2 symmetry, and is therefore weak; the next transition $2b_1 \rightarrow 2a_2$ is stronger. The same is true for the A_1 transitions, which correspond to $2b_1 \rightarrow 3b_1$ (weak) and $1a_2 \rightarrow 2a_2$ (strong). Therefore, the weakness of the HOMO-LUMO transition in thiophene can be understood as a relic of the (broken) D_{5h} symmetry in Fig. 7 we have plotted the calculated TDDFT optical gap as a function of the reciprocal chain length. As for the ionization potential, the calculated optical gap extrapolates for the oligomers to a polymer limit, which is too low in energy with respect to the experimental gap. The finite localization length of the electron-hole pair created in the excitation process can account for this discrepancy. This localization could

be intrinsic or is perhaps a consequence of structural defects or rotational disorder. Broken-symmetry solutions may correct a part of this problem and will be explored. But here too the deviations may be partly inherent to the TDDFT method used here, which does not take the self-energy correction properly into account.

In Fig. 7 we also display the TDDFT results for the lowest excited triplet state as a function of the reciprocal chain length. Comparing these results with the TDDFT for the singlet state one finds for the monomer a singlet-triplet splitting of 1.8 eV and this number is a direct measure for the exchange integral ($K=0.9$ eV). The moderate dependence of the value of the exchange splitting on the chain length for at least the smaller oligomers suggests that at least the triplet excitations are excitonic in nature with exciton sizes in the order of at most a few monomer units.

If we consider the molecular orbitals of the oligomers as being constructed from a linear combination of monomer thiophene orbitals, we can analyze the expectation value of the dipole operator in terms of on-site contributions and next-neighbor contributions. The on-site contribution, which in fact constitutes the HOMO-LUMO transition in the thiophene molecule, is weak as explained before and the next-neighbor contribution will be responsible for the increase of the oscillator strength with the chain length. Within this approximation and with a proper normalization of the wave functions, we can derive a simple expression for the value the oscillator strength f as a function of the transition dipole moment μ , chain length (N), and energy of the transition (ΔE):

$$f = \frac{2}{3} \left[\mu_{ii} + \mu_{ij} \left(2 - \frac{2}{N} \right) \right]^2 \Delta E. \quad (8)$$

For the larger oligomers we expect the oscillator strength of the HOMO-LUMO transition to behave like

$$f = f_{\text{polymer}} - \frac{\text{const}}{N}. \quad (9)$$

Here f_{polymer} is the oscillator strength of the infinite polymer. Figure 8 very clearly shows the dependence on $1/N$ of the oscillator strength from our TDDFT calculations.

In order to model the effects of rotational disorder and structural defects on the electronic properties of the oligothiophenes, we studied the ground- and excited-state properties of α -2T as a function of the dihedral angle between both monomer units. Chadwick and Kohler¹⁵ found experimental evidence of the coexistence of *cisoid* and *transoid* bithiophenes in a supersonic expansion. The ratio is dependent on the temperature of the expansion, and the enthalpy difference between the two structures was found to be 1.16 ± 0.13 kcal/mol. One should, of course, realize that the dihedral angles in the gas phase are 72° for the *cisoid* form and 64° for the *transoid* form,¹⁵ while those molecular structures are flat in the solid phase.³⁹ Because interaction between the molecules in the crystal are only weak, we expect a rather shallow potential well for torsion. In Fig. 9 we give the potential well for the *cis-trans* isomerization with the lowest energy for a flat *transoid* bithiophene structure. For the most

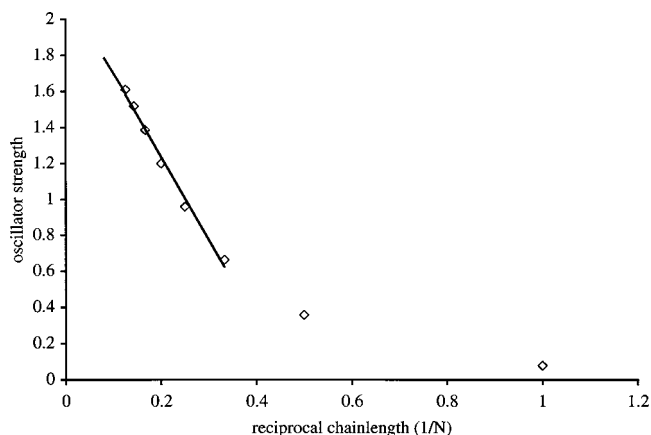


FIG. 8. Dependence of the oscillator strength obtained from TDDFT calculations for oligomers of thiophene on the reciprocal chain length ($1/N$). This figure clearly shows the linear dependency on $1/N$ for the larger oligomers.

stable *cisoid* structure the dihedral angle is around 70° , which is very close to experiment, the *transoid* conformation is 0.72 kcal/mol more stable than the *cisoid* conformation, and the transition state barrier is 4.13 kcal/mol.

In Fig. 10 we give the molecular orbital structure of bithiophene for torsion angles from 180° (*transoid*) to 0° (*cisoid*) (although we do in fact a calculation of the molecule in vacuum, we take the structural parameters for the molecule in the solid). In a tight-binding model the HOMO is built from an antibonding combination of the original thiophene $1a_2$ orbitals and the HOMO-3 from the bonding combination, and their splitting is dependent on the transfer or hopping integral. At 90° the two-ring systems are perpendicular, and the two π systems do not interact and the transfer integral $t=0$, the two orbitals cross, and the splitting is zero. The transfer integral is a function of the torsion angle Φ , $t(\Phi) = T \times \cos(\Phi)$.

We can describe the molecular orbitals derived from the $3b_1$ thiophene LUMO in a similar way. In a solid-state de-

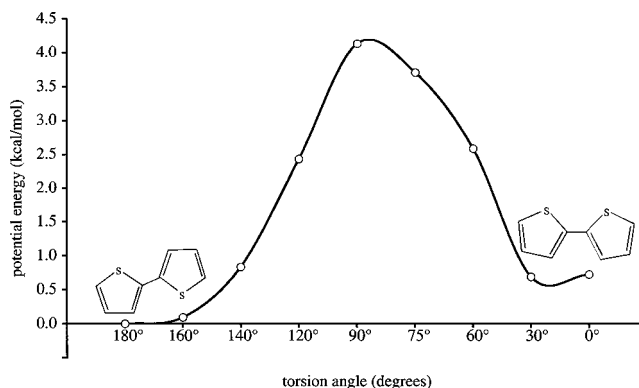


FIG. 9. Potential well for the *cisoid-transoid* isomerization as a function of the dihedral angle. This picture clearly shows a barrier of 4.3 kcal/mol for *cisoid-transoid* isomerization, and a small difference in stability of 1.16 kcal/mol between both isomers. For the *cisoid* isomer we find a minimum in energy for a nonplanar conformation. This should also be the case for the *transoid* isomer, but this would require a further geometry optimization.

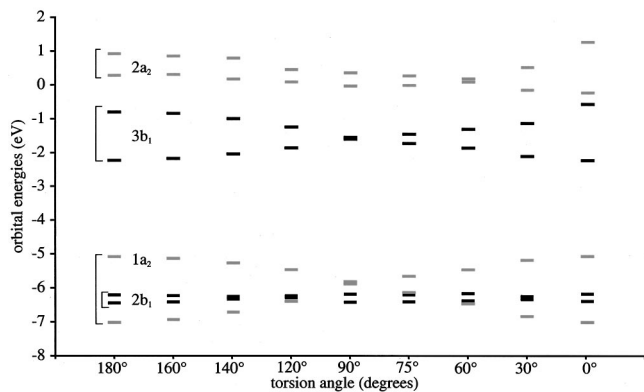


FIG. 10. Molecular-orbital structure of $\alpha-2T$ as a function of the dihedral angle.

scription this means that, upon torsion, the transfer integral decreases, the valence and conduction bands narrow, and the optical gap increases. For the thiophene $2b_{1-}$ and $2a_2$ -derived molecular orbitals, almost no dispersion is observed, and this can be attributed to the small transfer integral due to the small electron densities at the α carbon positions.

At 90° , where binding and antibinding orbitals become degenerate, the HOMO and LUMO are now both *twofold*-degenerate orbitals, each localized to one of the molecular entities. We have now a system of essentially noninteracting monomers, and we can analyze the optical spectrum in terms of pure intramolecular and intermolecular (charge-transfer) excitations.

The intramolecular excited states are expected to be almost degenerate, and the *gerade* combination will have small oscillator strength because of the corresponding weak monomer transition. The two charge-transfer-excited states are also expected to be close in energy, but will have no oscillator strength because of the two mutual perpendicular π systems. The energy splitting between the intramolecular and intermolecular excitations can in a tight-binding approach be interpreted as $U + \Delta U - V - 2K$, in which U is the on-site interaction and V the next-neighbor Coulomb interaction, ΔU the reduced screening of U due to end effects, and K the exchange integral.

Our TDDFT calculations are in excellent agreement with this simple model. At a dihedral angle of 90° we can identify two sets of two nearly degenerate transitions. At the low-energy end of the spectrum there are two almost degenerate intramolecular transitions at 4.65 eV, in which the *gerade* component has an oscillator strength of 0.295. About 1.0 eV higher in energy, we calculate two almost degenerate charge-transfer transitions at 5.63-eV energy, which as predicted do not carry any oscillator strength. From the splitting of the average intramolecular and intermolecular excitation energies we can estimate a value of 1.0 eV for $U + \Delta U - V - 2K$.

We have now extracted values for all the relevant parameters from the TDDTF calculations, which we will use as input parameters for a two-band model Hamiltonian calculation on the oligomers of size 1–6. We also can mimic the polymer limit by applying periodic boundary conditions to

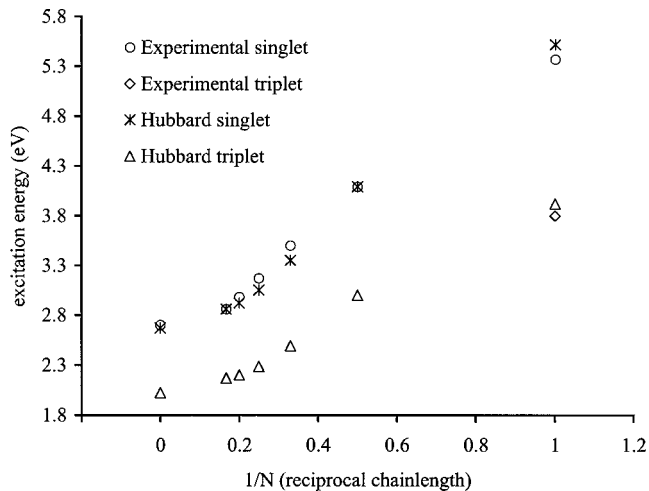


FIG. 11. The lowest singlet and triplet excited states obtained from a two-band Hubbard model Hamiltonian calculation with the parameter values given in Table I as a function of the reciprocal chain length ($1/N$). In the calculation we included only the ground state and all single excited states. Estimates for the polymer limit were obtained by imposing periodic boundary conditions on sexithiophene. For comparison available experimental data (Refs. 23, 24, and 27) (band maximum) are included.

an oligomer of size 6. In these calculations the ground state and single excited states were included. The doubly excited states are not important for the low-energy features because the relative large HOMO-LUMO splitting. In these calculations the input parameters mentioned above were further optimized until a good fit for the singlet and triplet optical gaps was obtained (Fig. 11). In order to obtain this result one has to take into account the reduced screening of the on-site Coulomb interaction on the terminal thiophene rings. With a static polarizability of about 10 \AA^3 for thiophene we estimated Δ at about 0.5 eV. The influence of the polarizability on the on-site coulomb interaction was already described in detail.⁴⁰ If this effect is not taken into account we find very

TABLE I. Values for the parameters used in a two-band Hubbard model Hamiltonian for a description of the electronic structure of the oligomers of thiophene. The values of the parameters given here are results of a fit to the experimental photoelectron spectroscopic and optical data (Refs. 23, 24, and 27). Starting values for the fit were obtained from the TDDFT calculations described in this paper.

Parameter	Value (eV)
U	2.4
ΔU	0.5
V	0.7
K	0.8
t_{hh}	-0.97
t_{ll}	0.76
t_{hl}	0.30
$\Delta\epsilon$	4.72

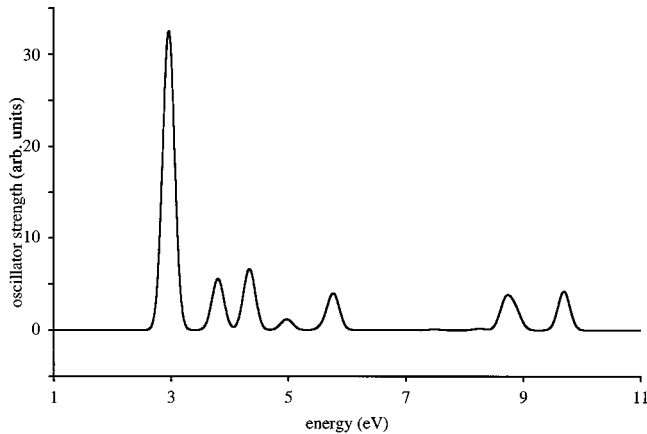


FIG. 12. The singlet optical spectrum of sexithiophene as obtained from a two-band Hubbard model Hamiltonian calculation; only the ground state and all single excited states are included. The values for the parameters given in Table I were used. Clearly visible is a bound excitonic state just below the conduction-band edge, which carries most of the spectral weight. In this calculation we have assumed equal transition dipole moments for the on-site and next-neighbor transitions.

low-energy excitonic states, with the electron on the terminal position and the hole next to it, this is due to the influence of the nearest-neighbor Coulomb interaction V , which lowers the energy of the electron hole pair if they are at the end of the chain.

The final set of parameters is given in Table I. From this we note the large value found for U of 2.4 eV, which is about half the bandwidth and sufficient to strongly bind even the singlet states into Frenkel-like excitons. In Fig. 12 we plot the singlet optical spectrum of sexithiophene: here for simplicity we assume equal transition dipole moments for the on-site and next-neighbor transitions. From this figure it is clear that the magnitude of the Coulomb interaction is sufficient to form a bound excitonic state in which the electron and hole are mainly on the same monomer as in a Frenkel exciton. Of course, for such a finite chain there is no real distinction between an exciton and an electron-hole pair, since they are always highly confined. In a subsequent paper we will show that these parameters indeed lead to Frenkel-like excitons for both the singlet and triplets, with the triplets much more tightly bound than the singlets.⁴¹

IV. CONCLUSIONS

In this paper it has been shown that the progression of the electronic properties with size for oligomers of thiophene can be understood in terms of a simple tight-binding model describing a linear system of weakly coupled monomer units, in which the building blocks mainly retain their molecular

identity. Because the HOMO and LUMO are very different in character, the first is *aromatic* with no sulfur character, and the latter is *quinoid* with significant density on the sulfur, one needs a two-band tight-binding approach in which the next-neighbor interaction is modeled with HOMO-HOMO, LUMO-LUMO, and intermolecular HOMO-LUMO transfer integrals. We have been able to extract a consistent set of tight-binding parameters from the results of the DFT calculations, which describe the experimental available data very well. It is surprising that a simple tight-binding Hamiltonian with only a monomer HOMO and a monomer LUMO gives such a good description of the details of the electronic structure of the oligomers of thiophene. Of course this may not be representative of other systems, especially polyacetylene. Further studies will explore the generality of this approach.

From TDDFT calculations on the lowest singlet and triplet excited states we could estimate an effective exchange integral of about 0.9 eV. The nature of the lowest singlet state can be analyzed in valence bond terms in intramolecular and intermolecular contributions. We showed that almost all the oscillator strength originates from intermolecular contributions, while the intramolecular contribution is weak. This finds its foundation in the fact that the electronic structure of the thiophene molecule is very similar to that of the isoelectronic cyclopentadienyl anion. This also explains the $1/N$ dependence of the magnitude of the oscillator strength for the larger oligomers.

We also found that rotational disorder is important in these systems, and that there is a very shallow potential well for torsion. These fluctuations will introduce an effective conjugation length, and most probably will be important in the localization of polarons and excitons, and may be an important source of traps in these materials.

For the dimer we showed that, if we take a torsion angle of 90° , the π systems will be perpendicular and the hopping integral will vanish. We are now left with two sets of excited states: one set of almost degenerate on-site excitations and one set of almost degenerate pure charge-transfer excitations. The splitting between both sets of excitations amounts to an effective on-site Coulomb interaction minus the next-neighbor Coulomb interaction $U + \Delta U - V - 2K$, and that splitting is about 1 eV.

From TDDFT calculations, numerical values could be extracted for the relevant physical quantities, which are the input parameters for the model Hamiltonian defined in this paper. After a full optimization we were able to realize an almost perfect fit for the singlet optical gap, and we predict the positions of triplet states for longer oligomers, for which they have not yet been observed to our knowledge. We show that electron correlation plays an important role in these systems, and that most of the optical spectral weight is carried by a singlet excitonic-like state, with an electron and hole concentrated on the same monomer or near-neighbor monomers.

- ¹J. Simon and J. J. Andréé, *Molecular Semiconductors* (Springer, Berlin, 1985).
- ²J. H. Burroughes, D. D. C. Bradley, A. R. Brown, R. N. Marks, K. Mackay, R. H. Friend, P. L. Burns, A. B. Holmes, *Nature* (London) **347**, 539 (1990).
- ³H. E. Katz, *J. Mater. Chem.* **7**, 369 (1990).
- ⁴*Handbook of Conducting Polymers*, edited by T. A. Skotheim (Dekker, New York, 1986).
- ⁵*Handbook of Oligo- and Polythiophenes*, edited by D. Fichou (Wiley-VCH, Weinheim, 1999).
- ⁶A. J. Heeger, S. Kivelson, J. R. Schrieffer, and W. P. Su, *Rev. Mod. Phys.* **60**, 781 (1988).
- ⁷J. W. Mintmire and C. T. White, *Phys. Rev. B* **27**, 1447 (1983).
- ⁸M. Chandross, Y. Shimoi, and S. Mazumdar, *Synth. Met.* **85**, 1001 (1997).
- ⁹R. J. Bursill, W. Barford, and H. Daly, *Chem. Phys.* **243**, 35 (1999).
- ¹⁰Z. C. Soos, S. Etemad, D. S. Galvao, and S. Ramasesha, *Chem. Phys. Lett.* **194**, 341 (1992).
- ¹¹J. W. van der Horst, P. A. Bobbet, P. H. L. de Jong, M. A. J. Michels, G. Brocks, and P. J. Kelley, *Phys. Rev. B* **61**, 15 817 (2000).
- ¹²M. Rohlfing and S. G. Louie, *Phys. Rev. Lett.* **82**, 1959 (1999).
- ¹³L. Serrano-Andrés, M. Merchán, M. Fülischer, and B. O. Roos, *Chem. Phys. Lett.* **211**, 125 (1993).
- ¹⁴M. H. Palmer, I. C. Walkera, and M. F. Guest, *Chem. Phys.* **241**, 275 (1999).
- ¹⁵J. E. Chadwick and B. E. Kohler, *J. Phys. Chem.* **98**, 3631 (1994).
- ¹⁶D. Birnbaum and B. E. Kohler, *J. Chem. Phys.* **96**, 2492 (1992).
- ¹⁷D. Birnbaum and B. E. Kohler, *J. Chem. Phys.* **90**, 3506 (1990).
- ¹⁸D. Birnbaum, D. Fichou, and B. E. Kohler, *J. Chem. Phys.* **96**, 165 (1992).
- ¹⁹B. E. Kohler, *Synth. Met.* **41-43**, 1215 (1991).
- ²⁰W. J. Buma, B. E. Kohler, and K. Song, *J. Chem. Phys.* **94**, 6367 (1991).
- ²¹K. Seki, U. O. Karlsson, R. Engelhardt, E. E. Koch, and W. Schmidt, *Chem. Phys.* **91**, 459 (1984).
- ²²D. Beljonne, Z. Shuai, and J. L. Brédas, *J. Chem. Phys.* **98**, 8819 (1993).
- ²³D. Jones, M. Guerra, L. Favaretto, A. Modelli, M. Fabrizio, and D. Distefano, *J. Phys. Chem.* **94**, 5761 (1990).
- ²⁴R. S. Becker, J. S. de Melo, A. L. Maçanita, and F. Elisei, *J. Phys. Chem.* **100**, 18 683 (1996).
- ²⁵F. Negri and M. Z. Zgiersky, *Chem. Phys.* **100**, 2571 (1994).
- ²⁶M. Rubio, M. Merchán, E. Ortí, and B. O. Roos, *J. Chem. Phys.* **102**, 3580 (1995).
- ²⁷J. C. Scaiano, R. W. Redmond, B. Mehta, and J. T. Arnason, *Photochem. Photobiol.* **52**, 655 (1990).
- ²⁸E. J. Baerends, D. E. Ellis, and P. Ros, *Chem. Phys.* **2**, 41 (1973).
- ²⁹G. te Velde and E. J. Baerends, *J. Comput. Phys.* **99**, 84 (1992).
- ³⁰C. F. Guerra, O. Visser, J. G. Snijders, G. te Velde, and E. J. Baerends, in *Methods and Techniques in Computational Chemistry*, edited by E. Clementi and C. Corongiu (STEF, Cagliari, Italy, 1995).
- ³¹S. H. Vosko, L. Wilk, and M. Nusair, *Can. J. Phys.* **58**, 1200 (1980).
- ³²S. J. A. van Gisbergen, J. G. Snijders, G. te Velde, and E. J. Baerends, *Comput. Phys. Commun.* **118**, 119 (1999).
- ³³S. J. A. van Gisbergen, J. G. Snijders, and E. J. Baerends, RESPONSE, extension of the ADF program for linear and nonlinear response calculations, with contributions by J. A. Groeneveld, F. Kootstra, and V. P. Osinga.
- ³⁴S. J. A. van Gisbergen Ph.D. thesis, Vrije Universiteit Amsterdam, 1998.
- ³⁵E. R. Davidson, *J. Comput. Phys.* **17**, 87 (1975).
- ³⁶E. R. Davidson, *Comput. Phys.* **7**, 5 (1993).
- ³⁷B. Liu (unpublished).
- ³⁸L. Noodleman, D. Post, and E. J. Baerends, *Chem. Phys.* **64**, 159 (1982).
- ³⁹J. Shinar, Z. Vardeny, E. Ehrenfreund, and O. Brafman, *Synth. Met.* **18**, (1987).
- ⁴⁰R. W. Lof, M. A. van Veenendaal, B. Koopmans, H. T. Jonkman, and G. A. Sawatzky, *Phys. Rev. Lett.* **68**, 3924 (1992).
- ⁴¹S. Yunoki, H. T. Jonkman, and G. A. Sawatzky (unpublished).